

Variational quantum mechanical and active database approaches to the rotational-vibrational spectroscopy of ketene, H₂CCO

Csaba Fábri,¹ Edit Mátyus,^{1,a)} Tibor Furtenbacher,¹ László Nemes,² Béla Mihály,^{1,3} Tímea Zoltáni,^{1,3} and Attila G. Császár^{1,b)}

¹Laboratory of Molecular Spectroscopy, Institute of Chemistry, Eötvös University, H-1518 Budapest 112, P.O. Box 32, Hungary

²Research Center for Chemistry of the Hungarian Academy of Sciences, H-1025 Budapest, Pusztaszeri út 59-67, Hungary

³Faculty of Chemistry and Chemical Engineering, Babeş-Bolyai University, Cluj-Napoca, Romania

(Received 3 March 2011; accepted 26 July 2011; published online 2 September 2011)

A variational quantum mechanical protocol is presented for the computation of rovibrational energy levels of semirigid molecules using discrete variable representation of the Eckart–Watson Hamiltonian, a complete, “exact” inclusion of the potential energy surface, and selection of a vibrational subspace. Molecular symmetry is exploited via a symmetry-adapted Lanczos algorithm. Besides symmetry labels, zeroth-order rigid-rotor and harmonic-oscillator quantum numbers are employed to characterize the computed rovibrational states. Using the computational molecular spectroscopy algorithm presented, a large number of rovibrational states, up to $J = 50$, of the ground electronic state of the parent isotopologue of ketene, H₂¹²C=¹²C=¹⁶O, were computed and characterized. Based on 12 references, altogether 3982 measured and assigned rovibrational transitions of H₂¹²C=¹²C=¹⁶O have been collected, from which 3194 were validated. These transitions form two spectroscopic networks (SN). The ortho and the para SNs contain 2489 and 705 validated transitions and 1251 and 471 validated energy levels, respectively. The computed energy levels are compared with energy levels obtained, up to $J = 41$, via an inversion protocol based on this collection of validated measured rovibrational transitions. The accurate inverted energy levels allow new assignments to be proposed. Some regularities and irregularities in the rovibrational spectrum of ketene are elucidated. © 2011 American Institute of Physics. [doi:10.1063/1.3625404]

I. INTRODUCTION

Up to a few years ago, the five-atomic ketene molecule was too large for an adequate determination of its rotational-vibrational spectrum via a variational quantum mechanical treatment employing an exact kinetic energy operator. It used to be possible to simulate high-resolution spectra of molecules of this size and larger only by the standard techniques of computational molecular spectroscopy,^{1–3} utilizing low-order perturbative approaches based on the Eckart–Watson (EW) (Refs. 4–6) Hamiltonians. These perturbative approaches result in approximate, effective Hamiltonians chosen with some arbitrariness through well-established and time-proven protocols. These empirical Hamiltonians have usually a relatively large number of fitting parameters to account for the required details of the measured spectra. This state of affairs proved to be quite unsatisfactory when the aim was to understand the low- and high-resolution molecular spectra of ketene isotopologues studied experimentally from the microwave to the infrared.^{7–43} The reason for the difficulties encountered is that these spectra exhibit several peculiar features resulting from the form of the associated ground electronic state potential energy surface (PES) of ketene.^{44,45}

These spectroscopic features, troublesome in a perturbational and empirical Hamiltonian approach though not in a variational one, have been summarized nicely by East *et al.*,⁴⁴ who performed one of the most careful *ab initio* studies of the spectral features of ketene, based on a quartic force field representation⁴⁶ of the PES and the traditional vibrational perturbation theory carried out to second order (VPT2).^{3,47–50}

The ketene molecule, H₂C=C=O, has an equilibrium structure of C_{2v} point-group symmetry in its electronic ground state (GS). It is a planar, semirigid asymmetric-top molecule, with a very large A rotational constant. As its Rayasymmetry parameter,⁵¹ $\kappa = -0.997$, suggests ketene is a near-prolate rotor. This determines the basic characteristics of the pure rotational and rotational-vibrational spectra of the ketene molecule. The principal axis a of the ketene molecule is oriented along the line of heavy atoms, while the c axis is perpendicular to the molecular plane. Thus, the dipole moment vector of ketene coincides with the a axis. Some of the complexities in the lower end of the high-resolution infrared spectrum of the parent ketene isotopologue arise because its three lowest fundamental vibrations [$\nu_5(B_1) \approx 587$, $\nu_6(B_1) \approx 526$, and $\nu_9(B_2) \approx 439$ cm⁻¹ in the Mulliken notation⁵²] cluster in the narrow 430–590 cm⁻¹ window. The next two fundamentals [$\nu_4(A_1) \approx 1116$ and $\nu_8(B_2) \approx 977$ cm⁻¹] occur again next to each other at about twice the frequency of the three bends (for the full set of fundamental vibrations of ketene, except the two C–H stretching modes not

^{a)}Present address: Laboratory of Physical Chemistry, ETH Zürich, Wolfgang-Pauli-Str. 10, CH-8093 Zürich, Switzerland.

^{b)}Author to whom correspondence should be addressed. Electronic mail: csaszar@chem.elte.hu.

investigated here, and the approximate motions involved, see Table III below). Complications also arise from the fact that there is a C_{2v} to C_s bifurcation on the ground-state PES of ketene, marking the advent of the out-of-plane bent (C_s^1) dissociation path when the C=C bond is elongated by just about 0.15 Å over its equilibrium value.⁴⁵ Furthermore, as the clustering of the fundamentals suggests, there are a number of vibrational (Fermi and Darling–Dennison) and rovibrational (Coriolis) resonances in different regions of the spectrum of ketene, occasionally causing localized level crossings distorting the rotational structures of some of the bands. A relevant example concerns the bands $3^1 \equiv \nu_3$ and $8^1 9^1 \equiv (\nu_8 + \nu_9)$.³⁵ Understanding the various resonances, detecting and assigning their spectral signatures, including irregular subband origins and unusual isotopic frequency shifts, and treating them with perturbative theoretical techniques meant that spectroscopists encountered severe difficulties while working on the measured spectra of ketene isotopologues and thus had to leave a considerable number of spectral features unassigned even at the low energies considered.

Still, as “the rich history of infrared and microwave studies of the ketene molecule is a microcosm of the development of modern spectroscopy,”⁴⁴ one can find a large number of studies employing perturbational techniques for the interpretation of the spectra of the ketene isotopologues. These studies were based on the original, in retrospect seemingly optimistic promise, that the spectrum of ketene “is difficult enough to be interesting but perhaps simple enough to be precisely analyzed.”¹² For example, a partial assignment of the coarse rotational structures of the four fundamentals below 1000 cm^{-1} (ν_5 , ν_6 , ν_8 , and ν_9) and analysis of the large first-order a -axis Coriolis perturbations is given in Refs. 23 and 32. An approach to the effective rotational constants to fit highly resolved J lines in the low-lying vibrational bands of ketene was reported in Ref. 42. In further studies of the vibration-rotation spectra of ketene, the accurate ground-state combination differences generated from ground-state rotational constants proved to be very useful.³⁹ During interpretation of almost all of the experimental studies resonances cause considerable difficulties, vibrational anharmonicity from spectroscopic analyses is known only to a limited extent even today. The different resonances have been theoretically analyzed by East *et al.*⁴⁴ pointing out many still existing difficulties with their interpretation and the scarcity of high-resolution studies of overtones and combination levels in several ketene isotopologues.

The most practical way out of the messy situation concerning the spectroscopy of ketene is to employ variational nuclear motion techniques. Nevertheless, to the best of our knowledge no variational studies, except that including our own preliminary results,⁵³ devoid of resonance problems have been reported for the spectra of ketene.

Apart from its spectroscopic significance, ketene as a model molecule has been serving as a testing ground for molecular structure determination methods,^{16,25,28,38,44} molecular force-field^{16,27,31,44} and PES computations and refinements,^{45,54} kinetic energy operator determinations,⁵⁵ and the elucidation of details of unimolecular reaction rate theories.^{45,56–60} Detailed knowledge of the rotational charac-

teristics of low-excitation vibrational bands has importance for model theories of molecular dissociation. Despite the large number of studies, ketene remains an intriguing molecule whose internal vibrational dynamics at excited vibrational levels is still essentially unknown. A step in this direction is provided by the present investigation.

It is well known that neither experiments nor first-principles (variational) computations can determine accurately in themselves the *complete* rotational-vibrational spectrum of small molecules even in a given region (say the infrared).⁶¹ Experiments provide accurate but extremely limited line and level information,^{62,63} while computations, due to the usually limited accuracy of the PESs,^{64–66} are unable to reach spectroscopic accuracy for all but the smallest systems.

It seems to us that the most practical approach to overcome most of the difficulties associated with the accuracy of the quantum mechanical approach and to gain an improved understanding of molecular spectra is to complement variational computation of the spectrum with a Hamiltonian-free, active information system approach.^{61,67} This requires building two databases linked together through a unique, but otherwise arbitrary, assignment and an inversion scheme. One of the databases contains the energy levels and the other the related transitions. Actually, this approach has a further advantage as through it one can take advantage of the strengths of the two main sources of spectroscopic information. Variational nuclear motion calculations can yield all the energy levels, with detailed assignment, and thus all the possible labeled transitions, though with limited accuracy. Experimental transitions and the energy levels obtained through an appropriately executed inversion procedure,^{67,68} have a much higher accuracy but are limited in number even in the spectroscopically most easily accessible and most studied regions. We do not see any other possible route to a more or less complete understanding of high-resolution spectra of medium-sized molecules than that sketched here and thus advocate the combined use of an active database approach what we call MARVEL, standing for Measured Active Rotational-Vibrational Energy Levels,⁶⁷ results from variational rovibrational computations and, of course, experimental information. This combined, three-legged approach is employed here for improving our understanding of the microwave and infrared spectra of the parent isotopologue of ketene. It is noteworthy that the same procedure can be employed almost verbatim for other (semirigid) molecules for which the quantum computations are technically feasible.

To achieve the general goals mentioned, the present study lays the foundation for an efficient variational quantum mechanical treatment of the vibrations and rotations of a molecule of the size of ketene and beyond, employing the Eckart–Watson Hamiltonian and arbitrary PESs. In particular, we present a computational molecular spectroscopy algorithm which allows the variational use of the exact rovibrational Eckart–Watson Hamiltonian, utilization of symmetry during the nuclear motion computations, elucidation of the symmetry features of rotational-vibrational wave functions, assignment of approximate zeroth-order (rigid rotor and harmonic oscillator) quantum numbers to the computed states, and determination of rovibrational states

for large J values even for polyatomic systems (Sec. II). In Sec. III, characteristics of the computational procedures employed for the case of ketene are summarized. Section IV details and discusses the results of the variational rovibrational computations. This study collected all the known and assigned experimental rovibrational transitions of the parent isotopologue of ketene available to us followed by the determination of the corresponding rovibrational energy levels via the MARVEL protocol. Section V provides a detailed discussion of these results. In Sec. VI, a few new assignments based on variational (DEWE), active database (MARVEL), and old experimental results are given. The paper ends with a summary of the new results and an outlook how the joint quantum mechanical and active database approach advocated here and employed for the example of ketene could be used in the future for other molecular systems for which the use of standard perturbational techniques proves to be overly difficult.

II. NUCLEAR MOTION COMPUTATIONS

After introducing the Born–Oppenheimer approximation^{69–71} to the rovibronic molecular Hamiltonian and solving the ensuing electronic motion problem, one obtains a PES (Refs. 65 and 66) which governs the motion of the nuclei. In recent papers,^{72,73} some of us proposed a variational first-principles nuclear motion algorithm named DEWE which computes vibrational levels of semirigid molecules with arbitrary PESs employing a single code. Since the detailed description of DEWE can be found in Refs. 72 and 73, only its key features are summarized here which also help to decipher the acronym: (a) DEWE employs a discrete variable representation⁷⁴ (D, the usual abbreviation is DVR) for the computation of the Hamiltonian matrix elements; (b) it is built upon the exact Eckart–Watson (EW) Hamiltonians; and (c) it allows for the exact (E) inclusion of an arbitrary potential energy surface. While the original DEWE code was capable to calculate only the pure vibrational levels of a given molecule, the algorithm presented hereby (Secs. II A and II B) enables the computation of rotational-vibrational energy levels for an arbitrary J rotational quantum number, which is a good quantum number in the absence of external fields and hyperfine interactions.

Due to the considerable expense of fully variational nuclear motion computations, it is clearly desirable to exploit molecular symmetry. Hereby a variant of the symmetry-adapted Lanczos (SAL) method^{75–77} has been implemented to compute rotational-vibrational energy levels with symmetry labels (Sec. II C). Based on a recent study,⁵³ it is discussed how the rovibrational states are labeled by traditional approximate rigid-rotor and harmonic oscillator quantum numbers (Sec. II D).

As the aim is the computation of (more or less) complete spectra, one needs to be able to determine highly excited rovibrational energy levels up to high values of the J rotational quantum number, which can be problematic even for four-atomic molecules. By increasing the value of J the size of the Hamiltonian matrix gets quickly very large and its spectrum gets very dense which also results in slower convergence of the iterative Lanczos eigensolver employed to obtain the re-

quired energy levels and wave functions within DEWE. This fact inspired us to propose an algorithm which successfully circumvents this problem by employing the direct product of the previously calculated $J = 0$ wave functions and rotational basis functions for the expansion of the rovibrational wave functions (Secs. II E and II F). This idea is related to a two-step procedure⁷⁸ advocated by Sutcliffe and Tennyson.

A. Rotational-vibrational energy levels and wave functions: DEWE

During the present study the Eckart–Watson form of the rovibrational molecular Hamiltonian⁴ was applied for the variational nuclear motion computations. The EW Hamiltonian has the following well-known form for an N -atomic molecule with a nonlinear reference configuration, expressed in orthogonal rectilinear coordinates,

$$\hat{H} = \frac{1}{2} \sum_{k=1}^{3N-6} \hat{P}_k^2 + \frac{1}{2} \sum_{\alpha,\beta} \mu_{\alpha\beta} (\hat{J}_\alpha - \hat{\pi}_\alpha)(\hat{J}_\beta - \hat{\pi}_\beta) - \frac{\hbar^2}{8} \sum_{\alpha} \mu_{\alpha\alpha} + \hat{V}, \quad (1)$$

where $\alpha, \beta = x, y, z$. Equation (1) is based on the Eckart embedding⁶ of the molecular frame, $\hat{P}_k = -i\hbar\partial/\partial Q_k$, where Q_k is the k th rectilinear (not necessarily normal) coordinate ($k = 1, \dots, 3N - 6$), \hat{J}_x, \hat{J}_y , and \hat{J}_z are the body-fixed components of the total angular momentum, $\hat{\pi}_\alpha$ refers to the components of the Coriolis coupling operator, $\mu_{\alpha\beta}$ stands for the elements of the generalized inverse inertia tensor, and \hat{V} is the potential energy operator.

The DEWE algorithm utilizes Hermite-DVR basis functions to set up the matrix representations of the operators $\hat{P}_k, \hat{\pi}_\alpha, \mu_{\alpha\beta}$, and \hat{V} . The full set of the necessary matrix elements of the vibrational part of the Hamiltonian is given in a previously published paper on the DEWE program package.⁷²

In order to set up the matrix representation of the \hat{H} rovibrational Hamiltonian, a suitable rotational basis has to be chosen. To facilitate symmetry considerations and avoid complex rovibrational matrix elements, it is worth combining the simple $|JKM\rangle$ symmetric-top eigenfunctions^{71,79} into a more sophisticated basis set. The DEWE algorithm utilizes the orthonormal Wang functions,^{71,79} satisfying both criteria, according to the following order:

$$\begin{aligned} & \frac{1}{\sqrt{2}} (|JKM\rangle + |J-KM\rangle), \text{ where } K \text{ is even,} \\ & \frac{1}{\sqrt{2}} (|JKM\rangle - |J-KM\rangle), \text{ where } K \text{ is odd,} \\ & \frac{i}{\sqrt{2}} (|JKM\rangle - |J-KM\rangle), \text{ where } K \text{ is even,} \\ & \frac{i}{\sqrt{2}} (|JKM\rangle + |J-KM\rangle), \text{ where } K \text{ is odd.} \end{aligned} \quad (2)$$

The four sets resulting from the use of the Wang functions correspond to the four irreducible representations

of the D_2 rotational group, applicable for asymmetric-top molecules. The matrix elements of the operators \hat{J}_x , \hat{J}_y , and \hat{J}_z in the primitive $|JKM\rangle$ basis and in the body-fixed frame can be expressed by means of angular momentum algebra. As known, the matrix representations of the $\hat{J}_\alpha \hat{J}_\beta$ operators can be given exactly by matrix multiplications of the \mathbf{J}_α and \mathbf{J}_β matrices.

After defining the rotational basis set one needs to consider the structure of the rovibrational Hamiltonian matrix,

$$\mathbf{H} = \mathbf{T}_v + \mathbf{T}_r + \mathbf{T}_{rv} + \mathbf{V}, \quad (3)$$

where the kinetic energy terms are defined by

$$\mathbf{T}_v = \mathbf{E}_{2J+1} \otimes \left(\frac{1}{2} \sum_{k=1}^{3N-6} \mathbf{P}_k^2 + \frac{1}{2} \sum_{\alpha,\beta} \boldsymbol{\mu}_{\alpha\beta} \boldsymbol{\pi}_\alpha \boldsymbol{\pi}_\beta - \frac{\hbar^2}{8} \sum_{\alpha} \boldsymbol{\mu}_{\alpha\alpha} \right), \quad (4)$$

$$\mathbf{T}_r = \frac{1}{2} \sum_{\alpha} \mathbf{J}_\alpha^2 \otimes \boldsymbol{\mu}_{\alpha\alpha} + \frac{1}{2} \sum_{\alpha < \beta} [\mathbf{J}_\alpha, \mathbf{J}_\beta]_+ \otimes \boldsymbol{\mu}_{\alpha\beta}, \quad (5)$$

$$\mathbf{T}_{rv} = - \sum_{\alpha,\beta} \mathbf{J}_\alpha \otimes (\boldsymbol{\mu}_{\alpha\beta} \boldsymbol{\pi}_\beta), \quad (6)$$

where \mathbf{E}_{2J+1} denotes the identity matrix of dimension $2J+1$ and $[\mathbf{J}_\alpha, \mathbf{J}_\beta]_+$ refers to the anticommutator of the matrices \mathbf{J}_α and \mathbf{J}_β . In the above equations, the truncated resolution of identity has been inserted amongst the $\boldsymbol{\mu}_{\alpha\beta}$, $\hat{\boldsymbol{\pi}}_\alpha$, and $\hat{\boldsymbol{\pi}}_\beta$ operators. As the $\boldsymbol{\pi}_\alpha$ matrices are purely imaginary, it is worth constructing purely imaginary \mathbf{J}_α matrices, which ensures that all of the \mathbf{J}_α^2 , $[\mathbf{J}_\alpha, \mathbf{J}_\beta]_+$, $\mathbf{J}_\alpha \otimes (\boldsymbol{\mu}_{\alpha\beta} \boldsymbol{\pi}_\beta)$, and $\boldsymbol{\pi}_\alpha \boldsymbol{\pi}_\beta$ matrices are real, resulting in a real rovibrational Hamiltonian.

B. Iterative eigensolver

The dimension of the rovibrational Hamiltonian equals $D(2J+1)$, where D is the number of vibrational basis functions. The DEWE algorithm employs the iterative Lanczos method^{80,81} to solve the eigenvalue problem of the Hamiltonian, which needs the evaluation of matrix-vector products. As D grows rapidly with the number of vibrational degrees of freedom, an effective matrix-vector product algorithm has been implemented, which does not need the Hamiltonian of rapidly growing dimension to be stored.

The shift-fold procedure of the family of polynomial spectral transformation techniques^{82,83} was employed during the Lanczos iterations to obtain the lowest eigenstates corresponding to the chosen Hamiltonian. Semi-orthogonality of the Lanczos vectors was maintained by using the periodic reorthogonalization algorithm,⁸⁴ whereby every second Lanczos vector is reorthogonalized against all the previous ones. The more sophisticated partial reorthogonalization technique^{85,86} resulted in a similar frequency of reorthogonalization steps as the periodic reorthogonalization, and thus the simpler periodic version was employed.⁷³ The thick-restart Lanczos method^{86,87} was used to compact the ever-growing Krylov subspace periodically.

TABLE I. Character tables of the isomorphic groups $C_{2v}(\mathbf{M})$ (molecular symmetry group), C_{2v} (point group), and D_2 (rotation group).

$C_{2v}(\mathbf{M})$ C_{2v}/D_2	$E(\mathbf{M})/E(\mathbf{P})$ $E(\mathbf{R})$	$(12)/C_2(z)$ R_z	$E^*/\sigma_v(yz)$ R_x	$(12)^*/\sigma_v(xz)$ R_y
$A_1/A_1/A$	1	1	1	1
$A_2/A_2/B_z$	1	1	-1	-1
$B_1/B_1/B_y$	1	-1	-1	1
$B_2/B_2/B_x$	1	-1	1	-1

C. The symmetry-adapted Lanczos method

Molecular symmetry can be exploited within the presented framework by adopting the symmetry-adapted Lanczos⁷⁵⁻⁷⁷ algorithm. Within this procedure the Lanczos vectors are projected onto the required irreducible representation of the molecular symmetry (MS) group. These projections, carried out during the course of the Lanczos iteration regularly, assure that the Lanczos algorithm will result in energy levels and wave functions of the given irreducible representation. The general implementation of this method for Abelian groups having $+1$ and -1 characters is summarized below.

Each element of the molecular symmetry group can be constructed as the product of a point-group and a rotational-group symmetry element.⁷¹ As the ketene molecule is examined in our current work, we focus on the structure of the $C_{2v}(\mathbf{M})$ MS group to which ketene belongs. The point group for ketene is C_{2v} , based on the symmetry of its equilibrium structure, while D_2 is the rotational symmetry group (rotation group) of ketene, an asymmetric top. Table I gives the character tables of the isomorphic $C_{2v}(\mathbf{M})$, C_{2v} , and D_2 groups of special relevance for this study.

If the equilibrium structure of ketene is placed into the yz plane and z coincides with the main CCO axis, the following equations relate the $C_{2v}(\mathbf{M})$ symmetry elements to the C_{2v} point-group and D_2 rotation-group elements (cf. Table I):

$$\begin{aligned} E(\mathbf{M}) &= E(\mathbf{P})E(\mathbf{R}), \\ (12) &= C_2(z)R_z, \\ E^* &= \sigma_v(yz)R_x, \\ (12)^* &= \sigma_v(xz)R_y. \end{aligned} \quad (7)$$

These relations are needed when the projector onto the i th irreducible representation is constructed by considering

$$\hat{P}_i = \frac{1}{h} \sum_{\hat{A} \in G} \chi_i(\hat{A}) \hat{A}, \quad (8)$$

where G is the molecular symmetry group, h is the order of G , and $\chi_i(\hat{A})$ is the character of the MS group element \hat{A} associated with the i th irreducible representation. The effect of \hat{P}_i on the original Lanczos vector \mathbf{x} is given by

$$\mathbf{x}_i = \mathbf{P}_i \cdot \mathbf{x}, \quad (9)$$

where \mathbf{x}_i is the projected Lanczos vector and \mathbf{P}_i is the matrix representation of the \hat{P}_i projector in the rovibrational basis.

As the current implementation applies only to Abelian groups, having characters $+1$ and -1 , the effect of a \hat{B}

point-group symmetry element on the Q_i normal coordinate is

$$\hat{B}Q_i = \chi_j(\hat{B})Q_i, \quad (10)$$

where Q_i forms the basis of the j th irreducible representation and the $\chi_j(\hat{B})$ character refers to the j th irreducible representation. According to Eq. (10), one can deduce the effect of \hat{B} on the $f_n(Q_i)$ one-dimensional Hermite-DVR vibrational basis functions as

$$\begin{aligned} \hat{B}f_n(Q_i) &= f_n(\hat{B}^{-1}Q_i) = f_n(Q_i), \text{ if } \hat{B}Q_i = Q_i, \text{ or} \\ \hat{B}f_n(Q_i) &= f_n(\hat{B}^{-1}Q_i) = f_n(-Q_i) = f_{-n}(Q_i), \text{ if } \hat{B}Q_i = -Q_i, \end{aligned} \quad (11)$$

where the $f_n(Q_i)$ one-dimensional functions were given the $n = -p, \dots, -1, 1, \dots, p$ or $n = -p, \dots, 0, \dots, p$ indices for $2p$ even and $2p+1$ odd numbers of basis functions, respectively, thus the $f_n(Q_i)$ basis functions are enumerated according to the ascending order of the Hermite-DVR grid points. Equation (11) is a direct consequence of the application of Hermite-DVR vibrational basis functions. In light of these equations, the following relation holds:

$$\begin{aligned} \langle f_m(Q_i) | \hat{B}f_n(Q_i) \rangle &= \langle f_m(Q_i) | f_n(Q_i) \rangle = \delta_{mn}, \text{ if } \hat{B}Q_i = Q_i, \\ \langle f_m(Q_i) | \hat{B}f_n(Q_i) \rangle &= \langle f_m(Q_i) | f_{-n}(Q_i) \rangle = \delta_{m,-n}, \text{ if } \hat{B}Q_i = -Q_i. \end{aligned} \quad (12)$$

According to Eq. (12), the matrix representation of \hat{B} in the basis of Hermite-DVR functions is either an identity or an anti-diagonal matrix. Since the vibrational basis is constructed as the direct product of one-dimensional Hermite-DVR functions, the matrix representation of \hat{B} is the direct product of the related matrices. This operation results in the matrix representation of \hat{B} which is a permutation matrix and has the dimension of the direct product vibrational basis.

For the construction of the matrix representation of a \hat{C} rotation-group (D_2) symmetry element, it is important to know the symmetry properties of the Wang functions defined by Eq. (2). The Wang-functions are basis functions of the irreducible representations of the Abelian D_2 rotation group.⁷¹ Thus, the matrix representation of \hat{C} is diagonal and has +1 or -1 in its main diagonal:

$$\langle W_m(\mathbf{\Omega}) | \hat{C}W_n(\mathbf{\Omega}) \rangle = \chi_n(\hat{C})\delta_{mn}, \quad (13)$$

where $W_n(\mathbf{\Omega})$ refers to the $2J+1$ Wang functions for a given J , $\mathbf{\Omega}$ stands for the three rotational coordinates, and $\chi_n(\hat{C})$ is the character of \hat{C} in the irreducible representation spanned by $W_n(\mathbf{\Omega})$.

According to these arguments, the matrix representation of the $\hat{A} = \hat{B}\hat{C}$ molecular symmetry group element is given by the direct product of the previously derived matrix representations of \hat{C} and \hat{B} . Once the matrix representations of the MS group symmetry elements are available, one can construct the matrix of \hat{P}_i projectors by taking appropriate linear combinations of these \hat{A} matrices, see Eq. (8). As the \hat{P}_i projectors are represented by permutation matrices, an effective matrix-vector multiplication subroutine can be developed for evaluating the necessary $\mathbf{x}_i = \mathbf{P}_i \cdot \mathbf{x}$ products without having to construct and store the \mathbf{P}_i matrix explicitly.

This scheme does not decrease the size of the Hamiltonian matrix to be treated. Nevertheless, a considerable advantage of SAL is that the eigenvalues to be determined become considerably sparser resulting in an improved convergence of the Lanczos procedure and that symmetry labels are distributed automatically to the computed rovibrational states.

D. Assignment of rovibrational states: NMD and RRD

The normal mode decomposition (NMD) and rigid rotor decomposition (RRD) algorithms⁵³ were implemented in the DEWE program package in order to facilitate the assignment of zeroth-order harmonic oscillator (HO) and rigid rotor (RR) quantum numbers to the computed variational rovibrational eigenstates.

In the case of the NMD, overlaps between the ϕ_j variational vibrational and the ϕ_i^{HO} harmonic oscillator wave functions are to be computed. The NMD coefficient is defined as

$$c_{ji} = |\langle \phi_i^{\text{HO}} | \phi_j \rangle|^2. \quad (14)$$

Labeling of the ϕ_i variational vibrational wave functions with approximate HO quantum numbers can be accomplished by finding the dominant NMD coefficient given by Eq. (14).

After generating the NMD coefficients and HO quantum numbers, one can move forward to label the variational rotational-vibrational eigenstates with HO and RR quantum numbers. The J rotational quantum number is exact and one of the input parameters of the DEWE program package. Determination of the approximate K_a and K_c labels necessitates the computation of the

$$\langle \psi_i | \phi_j R_k \rangle \quad (15)$$

overlaps, where ψ_i is a variational rovibrational, ϕ_j a variational vibrational, and R_k a rigid rotor wave function. After finding the dominant $\phi_a R_b$ contribution in ψ_i , it is straightforward to assign ψ_i with the HO labels of ϕ_a and K_a and K_c labels of R_b .

E. Computation of high- J rovibrational states: DEWE-VS

Determination of the large number of rovibrational states associated with large J values is extremely demanding along the traditional procedures (described in Sec. II A). Here we present a technique employing a vibrational subspace (VS), which can be used for the determination of a large number of rovibrational energies and is almost cost free.

The rotational-vibrational Hamiltonian can be partitioned as

$$\hat{H} = \hat{T}_v + \hat{T}_r + \hat{T}_{rv} + \hat{V} = \hat{H}_v + \hat{T}_r + \hat{T}_{rv}, \quad (16)$$

where

$$\hat{H}_v = \hat{T}_v + \hat{V} \quad (17)$$

is the vibration-only Hamiltonian. After solving the

$$\hat{H}_v \phi_i = E_i \phi_i \quad (18)$$

vibrational Schrödinger equation and obtaining the ϕ_i vibrational states and the corresponding E_i vibrational energy levels, a subset of the ϕ_i functions can be employed as a compact vibrational basis for the rotational-vibrational computations. In order to construct a new and very compact rovibrational basis, consider the direct product of the ϕ_i vibrational states and some R_k rotational basis functions for a given J ,

$$\{\phi_i R_k\}, \text{ where } i = 1, \dots, n \text{ and } k = 1, \dots, 2J+1. \quad (19)$$

The matrix representation of \hat{H}_v is diagonal,

$$\langle \phi_i R_j | \hat{H}_v | \phi_k R_l \rangle = E_i \delta_{ik} \delta_{jl}. \quad (20)$$

The necessary matrix elements of the $\hat{\pi}_\alpha$ and $\mu_{\alpha\beta}$ operators in the basis of the ϕ_i vibrational states can be deduced based on previously published papers on the DEWE algorithm.^{72,73} There are several choices for defining the $2J+1$ R_k rotational basis functions for a given J : (a) simple $|JKM\rangle$ functions, (b) Wang functions (see Eq. (2) for their definition), and (c) rigid-rotor eigenfunctions. We chose the third option, namely, the $2J+1$ rigid-rotor eigenfunctions computed with equilibrium rotational constants were utilized as a rotational basis, as this choice gives rise to a very straightforward computation of the RRD coefficients.

This new contraction-like technique, denoted as DEWE-VS, exhibits the following significant advantages: (a) the vibrational subspace is very compact (it consists of typically the first few hundred VBOs of the molecule), which results in a Hamiltonian of modest size even for high J values; (b) the RRD analysis, which facilitates the labeling of the variationally computed rovibrational states, is especially simple, as the RRD coefficients are equal to the absolute squares of the components of the eigenvectors of the rotational-vibrational Hamiltonian; (c) the vibrational basis functions are automatically symmetry adapted (as they are basis functions of the irreducible representations of the point group), which facilitates the exploitation of molecular symmetry during the computation; (d) once the necessary vibrational matrix elements for the construction of the representation of \hat{T}_r and \hat{T}_{rv} have been computed, they can be saved in a file of modest size for later use, which greatly reduces the cost of the further computations; and (e) due to the modest size of the final Hamiltonian one can use direct eigensolvers instead of the iterative Lanczos algorithm; thus, the spectral density of the rovibrational energy levels does not affect the convergence speed of the diagonalization (for larger matrices one can, of course, return to Lanczos techniques). For this study, a parallel eigensolver of the Math Kernel Library⁸⁸ was chosen.

F. Symmetry considerations during the VS rotational-vibrational procedure

As in the present application, the new rotational-vibrational procedure of Sec. II E, DEWE-VS, does not utilize the Lanczos eigensolver, an additional algorithm is needed

for the symmetry classification of the rotational-vibrational energy levels and wave functions. For Abelian groups having $+1$ and -1 characters, the symmetry labels can be generated by simple analysis of the rotational-vibrational wave functions expanded in the basis defined by Eq. (19). This analysis builds upon the following: (a) only Abelian molecular symmetry groups having $+1$ or -1 characters are considered; (b) the vibrational basis consists of the vibrational states of the molecule which are basis functions of the irreducible representations of the point group; (c) the rotational basis consists of the rigid-rotor eigenfunctions which are basis functions of the irreducible representations of the rotation group (D_2 for asymmetric tops); and (d) symmetry elements of the molecular symmetry group are products of point-group and rotation-group elements (see Sec. II C for a more detailed description). If an arbitrary \hat{A} MS operator is given by

$$\hat{A} = \hat{B}\hat{C}, \quad (21)$$

where \hat{B} is a point-group (PG) and \hat{C} is a rotation-group (RG) element, the effect of \hat{A} on a $\phi_i R_k$ basis function is the following:

$$\begin{aligned} \hat{A}(\phi_i R_k) &= (\hat{B}\phi_i)(\hat{C}R_k) = \chi_b^{\text{PG}}(\hat{B})\chi_c^{\text{RG}}(\hat{C})\phi_i R_k \\ &= \chi_a^{\text{MS}}(\hat{A})\phi_i R_k, \end{aligned} \quad (22)$$

where a , b , and c refer to the irreducible representations of the molecular symmetry, point, and rotation groups, respectively, and

$$\hat{B}\phi_i = \chi_b^{\text{PG}}(\hat{B})\phi_i \quad (23)$$

and

$$\hat{C}R_k = \chi_c^{\text{RG}}(\hat{C})R_k, \quad (24)$$

as all the groups are Abelian. In view of these equations, it is evident that the $\phi_i R_k$ (where $i = 1, \dots, n$ and $k = 1, \dots, 2J+1$) functions are basis functions of the one-dimensional irreducible representations of the molecular symmetry group.

After finding the dominant $\phi_i R_k$ contribution in the variational expansion of the rotational-vibrational wave functions the characters of the irreducible representation spanned by this $\phi_i R_k$ are to be computed for all the conjugacy classes according to Eq. (22). The symmetry species of a given rovibrational state is obviously the same as that of the dominant $\phi_i R_k$ contribution.

III. COMPUTATIONAL DETAILS

A. Model of the PES

The empirically adjusted *ab initio* quartic internal coordinate force field of Ref. 44 was employed in this study as a model of the PES of ketene around the equilibrium structure. This simple representation of the ground-state PES of ketene was obtained by East *et al.*⁴⁴ as a result of two cycles of refinements. In the interior cycle A, the harmonic (quadratic) part of the force field was refined by scaling it according to the scaled

quantum mechanical force field recipe^{89,90} to harmonized frequencies, obtained via the VPT2 protocol, while keeping the reference (equilibrium) geometry fixed. In the exterior cycle B, corrections to the rotational constants based on lowest-order vibration-rotation interaction constants computed from the actual cubic force field, augmented with small centrifugal distortion and electronic corrections, were applied to the experimental ground-state rotational constants in order to get an improved estimate of the equilibrium molecular structure of ketene. The exterior and interior cycles were repeated until self-consistency was achieved, resulting in a quartic force field which reproduced the available experimental fundamentals *within the VPT2 protocol* by about 1 cm^{-1} on average.

In order to make the internal coordinate quartic force field of Ref. 44 optimal for use in variational nuclear motion computations,⁹¹ the simple stretching coordinates were replaced by Simons–Parr–Finlan coordinates.⁹² The necessary nonlinear transformations were performed analytically by employing the INTDER2000 program system.^{93–95} The final quartic internal coordinate force field employed in this study is defined in the supplementary material.⁹⁶

B. Rovibrational states

All the nuclear motion computations utilized the latest version of the in-house DEWE program package written in FORTRAN90. The atomic masses employed for all the computations are $m(\text{H}) = 1.007825\text{ u}$, $m(^{12}\text{C}) = 12.000000\text{ u}$, and $m(^{16}\text{O}) = 15.994910\text{ u}$. The reference structure and the definition of the rectilinear coordinates are given in the supplementary material⁹⁶ facilitating reproduction of the results of the present study. Following a considerable number of test computations, the vibrational basis was chosen as follows for the results reported hereby: 6, 8, and 10 basis functions for the four stretching motions, the two highest bends, and the three lowest bends, respectively. The size of the corresponding vibrational Hamiltonian thus became 82 944 000. This basis allowed execution of vibration-only computations on a personal computer within a few weeks resulting in the lowest 100 eigenvalues and eigenfunctions. 4218 matrix-vector multiplications and 73 restarts were necessary in the Lanczos routine for obtaining these results.

The rotational-vibrational computations were performed in two different ways. First, the DEWE algorithm of Sec. II A was employed up to $J = 3$ with a vibrational basis of 21 781 872 functions (7 basis functions for the five bends and 6 for the four stretching motions). Second, the procedure of Sec. II E (DEWE-VS) was applied for the computation of rotational-vibrational energy levels up to $J = 50$ (for a list of rovibrational states corresponding to the first four VBOs, GS, $\nu_9 = 9^1$, $\nu_6 = 6^1$, and $\nu_5 = 5^1$, see supplementary material⁹⁶). During the DEWE-VS computations, the previously mentioned lowest 100 vibrational wave functions defined the vibrational subspace employed.

TABLE II. Data sources for line information and their characteristics for $\text{H}_2^{12}\text{C}=\text{C}=\text{O}$ employed during the present MARVEL analysis.

Tag	Range (cm^{-1}) ^a	Trans. (A/V) ^b
77FaKrMu [26]	0.013–0.038	2/2
03GuHu [20]	0.076–10.882	97/65
52JoSt [12]	0.264–2.041	29/24 ^c
72JoStWi [19]	0.264–6.123	53/45
01SuDr [35]	0.674–0.674	1/1
63CoEs [13]	0.674–1.361	15/9
90BrGoMcPi [25]	0.674–12.140	37/20
92JoNeYaWa [39]	0.692–24.445	146/77
96HiZeDoGu [40]	1.337–5.445	130/89
11FaMaFuNe ^d	332.638–1021.930	2345/1945
94EsDoCaOr [9]	3049.661–3089.528	276/175
03StNeGr [24]	4269.605–6271.494	851/742

^aNote that (a) the range indicated does not mean the actual spectral range covered by the experiment but simply the lowest- and highest-energy transition present in the database and (b) the ranges are not always indicative of the vibrational states covered by the experiment.

^bTrans. = transitions, A = available in the original data source, V = validated by MARVEL during the present work.

^cThe 52JoSt.24 transition was removed manually from the database as it has the same lower and upper level assignments in the original publication.

^dThis work. All these transitions have been used in previous publications on the spectroscopy of ketene but never reported explicitly.

The NMD and RRD analyses of the computed rovibrational wave functions were performed according to the recipes of Ref. 53.

C. MARVEL analysis

The MARVEL analysis of the measured rovibrational transitions employed the latest version of the in-house program MARVEL (Ref. 67) written in C++.

In order to keep the experimental sources of the measured transitions data employed tractable, each experimental source received a tag (see Table II). The technical description of the tags is given in the supplementary material.⁹⁶ These tags are used throughout this work. Table II contains the intervals characterizing the measured transitions as well as the number of the available (A) and validated (V) transitions present in a given source.

We could not use the several hundred assigned transitions in 87DuFeHaToa,³⁶ as not the individual transitions but the effective spectroscopic constants deduced from them were reported in the paper. We did, however, employ many previously assigned but so far unpublished high-resolution mid-infrared transitions,⁹⁷ which became part of the present work and thus received the tag 11FaMaFuNe (see Table II). There are many pure rotational transitions reported in the Cologne Database for Molecular Spectroscopy (CDMS),⁴³ which come from several known sources.^{12, 16, 20, 25, 26, 39} Thanks to the kind help of Dr. Müller, maintaining the CDMS, these transitions received their original tag and at the end no explicit reference is made in the MARVEL input to the CDMS. Transitions reported in Ref. 20 are also listed under their original sources in the MARVEL input file.

Due to the symmetry of the molecule, the rotational-vibrational energy levels of ketene form two spectroscopic

TABLE III. Active database (MARVEL) and variational quantum mechanical (DEWE) vibrational band origins (VBO, cm^{-1}) for $\text{H}_2^{12}\text{C}=\text{C}=\text{C}=\text{O}$ in order of increasing energy, with zeroth-order normal-mode (NMD) assignments, symmetry labels (Sym.), and MARVEL uncertainties (Unc., 10^{-6}cm^{-1}). The number of validated rotational-vibrational levels (RL) associated with the vibrational bands in the present database and traditional characterization of the fundamentals are also given.

Label	Sym.	MARVEL	Unc. ^a	RL	DEWE ^b	Characterization
GS	A_1	0	0	329	6832.0	Ground state
9^1	B_2	439.386511	235	148	437.1	In-plane C=C=O bend
6^1	B_1	526.070043	236	248	534.0	Out-of-plane C=C=O bend
5^1	B_1	587.428312	231	200	603.5	CH_2 wag
9^2	A_1				873.8	
8^1	B_2			234	972.6	CH_2 rocking
$6^1 9^1$	A_2				975.0	
$5^1 9^1$	A_2				1047.1	
6^2	A_1				1071.7	
4^1	A_1				1113.3	
$5^1 6^1$	A_1				1169.1	
5^2	A_1				1211.4	
9^3	B_2				1310.1	
3^1	A_1				1402.3	CH_2 scissor ^c
$6^1 9^2$	B_1				1412.4	
$8^1 9^1$	A_1				1415.9	
$5^1 9^2$	B_1				1490.5	
$6^1 8^1$	A_2				1508.2	
$6^2 9^1$	B_2				1516.2	
$4^1 9^1$	B_2				1558.2	
$5^1 8^1$	A_2				1567.3	
6^3	B_1				1607.2	
$5^1 6^1 9^1$	B_2				1612.7	
$4^1 6^1$	B_1				1637.7	
$5^2 9^1$	B_2				1659.0	
$4^1 5^1$	B_1				1702.3	
^d	B_1				1714.8	
9^4	A_1				1745.9	
^d	B_1				1784.2	
5^3	B_1				1808.0	
$8^1 9^2$	B_2				1836.0	^e
$6^1 9^3$	A_2				1847.0	
$3^1 9^1$	B_2				1854.2	^e
$5^1 9^3$	A_2				1933.6	
8^2	A_1				1940.9	
$6^1 8^1 9^1$	B_1				1943.3	
$6^2 9^2$	A_1				1953.2	
$3^1 6^1$	B_1				1966.9	
$4^1 9^2$	A_1				2001.0	
$5^1 8^1 9^1$	B_1				2013.2	
$6^2 8^1$	B_2				2044.9	
$6^3 9^1$	A_2				2051.0	
$5^1 6^1 9^2$	A_1				2052.1	
$3^1 5^1$	B_1				2077.8	
$4^1 8^1$	B_2				2080.1	
$4^1 6^1 9^1$	A_2				2085.9	
$5^2 9^2$	A_1				2108.1	
6^4	A_1				2133.6	
$5^1 6^1 8^1$	B_2				2133.6	
^d	A_2				2147.5	
2^1	A_1				2153.7	C=O stretch
$5^2 8^1$	B_2				2161.5	
$4^1 6^2$	A_1				2162.9	

TABLE III. (*Continued*)

Label	Sym.	MARVEL	Unc. ^a	RL	DEWE ^b	Characterization
^d	A_2				2166.9	
9^5	B_2				2178.1	

^aThe uncertainties (Unc.) are given in units of 10^{-6}cm^{-1} . VBOs not determined by the experimental data available are left blank in the MARVEL and Unc. columns. Two further MARVEL VBOs have been determined as part of the present analysis: $1^2 (A_1) = 6068.373106(50)$ and $7^2 (A_1) = 6262.909106(50) \text{cm}^{-1}$, holding 130 and 59 RLs, respectively. The 1^1 , 8^1 , $1^1 7^1$, and 2^2 VBOs could not be determined via the MARVEL analysis but in the present database they hold 107, 234, 201, and 65 RLs, respectively.

^bThe vibrational basis was chosen as follows for the VBOs computed by DEWE: 6, 8, and 10 basis functions for the four stretching motions, the two highest bends, and the three lowest bends, respectively.

^cThere is a very strong mixing between the 3^1 and $8^1 9^1$ states (see Table IV), in fact for this state 3^1 and $8^1 9^1$ have NMD contributions of 43% and 50%, respectively.

^dNo reasonable assignment can be given due to extremely heavy mixing of several states.

^eNote the very strong mixing of the $8^1 9^2$ and $3^1 9^1$ states.

networks (SN).⁹⁸ There are no ortho-para transitions measured.

Since the MARVEL energy levels determined do not have the same dependability (the uncertainties resulting from the least-squares fit cannot always be trusted, especially when the energy level is determined by a single transition), we attached quality classifications to the levels, distributing them into three categories: A (best), B, and C (worst). For details concerning these classifications see the supplementary material.⁹⁶

IV. VARIATIONAL ROVIBRATIONAL ENERGY LEVELS

A. Vibrational band origins

The vibrational energy levels computed with the DEWE program package are collected in Table III. Since the present quartic force field does not take into account the dissociation path bifurcation occurring on the ground-state PES of ketene at about 4000cm^{-1} , we report computed vibrational band origins (VBO) only up to about 2200cm^{-1} , i.e., up to the neighborhood of the C=O stretch fundamental $2^1 = \nu_2(A_1)$. The NMD (Ref. 53) tables of the parent isotopologue of ketene, close to the same energy cutoff value, are reported in Tables IV–VII for the four irreducible representations of the C_{2v} point group.

The very strong mixing within some of the vibrational states of ketene is clearly evident from the NMD data of Tables IV–VII. Therefore, the zeroth-order normal-mode labeling given in Table III becomes rather approximate in certain cases even at the low energies and low excitations considered. The most striking example concerns the A_1 -symmetry states at 1402.3 and 1415.9cm^{-1} (variational results), which have an almost perfect 50-50 mixing of the ω_3 and $(\omega_8 + \omega_9)$ harmonic oscillator basis states. This means that it is unclear, based on the present variational quantum chemical computations, whether the $3^1 = \nu_3(A_1)$ fundamental of parent ketene is at 1402 or at 1416cm^{-1} . The NMD analysis prefers the higher assignment by NMD coefficients 50 to 43. However, we prefer the lower assignment though clearly this is somewhat arbitrary and can be supported only if comparison with experimental and harmonic results is considered. The strong

TABLE V. The lowest-energy part of the normal-mode decomposition (NMD) table of ketene for A_2 point-group symmetry.

NMD (ν, ω) ^{a,b}		936.2	1015.5	1498.6	1577.9	1803.4	1882.7	1941.4	2020.7	2082.2	2100.0	2161.5	2179.3	2351.4	2365.8	2430.7	2445.1	2503.8	2583.1	2644.6	2662.4	2670.6	2723.9	2741.7	2749.9	2808.6	2887.9	2913.8		
		$\omega_6+\omega_8$	$\omega_5+\omega_8$	$\omega_6+\omega_8$	$\omega_5+\omega_8$	$\omega_6+3\omega_8$	$\omega_5+3\omega_8$	$3\omega_6+\omega_8$	$\omega_5+2\omega_6+\omega_8$	$\omega_4+\omega_6+\omega_8$	$2\omega_5+\omega_6+\omega_8$	$\omega_4+\omega_5+\omega_8$	$3\omega_5+\omega_8$	$\omega_5+\omega_6+\omega_8$	$\omega_6+\omega_8+2\omega_8$	$\omega_5+\omega_8+\omega_8$	$\omega_5+\omega_8+2\omega_8$	$3\omega_6+\omega_8$	$\omega_5+2\omega_6+\omega_8$	$\omega_4+\omega_6+\omega_8$	$2\omega_5+\omega_6+\omega_8$	$\omega_6+5\omega_8$	$\omega_4+\omega_5+\omega_8$	$3\omega_5+\omega_8$	$\omega_5+5\omega_8$	$3\omega_6+3\omega_8$	$\omega_5+2\omega_6+3\omega_8$	$\omega_5+\omega_6+\omega_8$	N	
975.0	ψ_6	94	1	0	0	0	0	0	0	0	0	0	0	0	0	0	0	0	0	0	0	0	0	0	0	0	0	0	0	97
1047.1	ψ_7	1	94	0	0	0	0	0	0	0	0	0	0	0	0	0	0	0	0	0	0	0	0	0	0	0	0	0	0	96
1508.2	ψ_{17}	0	0	93	2	0	0	0	0	0	0	0	0	0	0	0	0	0	0	0	0	0	0	0	0	0	0	0	0	97
1567.3	ψ_{20}	0	0	2	94	0	0	0	0	0	0	0	0	0	0	0	0	0	0	0	0	0	0	0	0	0	0	0	0	96
1847.0	ψ_{31}	0	0	0	0	82	0	1	0	4	0	0	0	1	0	0	0	0	0	0	0	0	0	0	0	0	0	0	0	90
1933.6	ψ_{33}	0	0	0	0	1	81	0	0	0	1	5	1	0	0	0	0	0	0	0	0	0	0	0	0	0	0	0	0	91
2051.0	ψ_{41}	0	0	0	0	1	0	74	2	2	0	0	0	8	0	0	0	0	0	0	0	0	0	0	0	0	0	0	0	91
2085.9	ψ_{45}	0	0	0	0	3	1	0	28	56	1	0	0	0	1	1	0	0	0	0	0	0	0	0	0	0	0	0	0	93
2147.5	ψ_{49}	0	0	0	0	1	2	0	26	12	7	33	2	2	0	2	0	0	0	0	0	0	0	0	0	0	0	0	0	89
2166.9	ψ_{53}	0	0	0	0	0	3	0	21	20	22	23	1	2	0	0	1	0	0	0	0	0	0	0	0	0	0	0	0	94
2230.0	ψ_{56}	0	0	0	0	0	1	0	0	0	49	29	1	1	0	3	0	0	0	0	0	0	0	0	0	0	0	0	0	88
2266.8	ψ_{58}	0	0	0	0	0	1	0	0	0	1	5	81	0	0	0	0	0	0	0	0	0	0	0	0	0	0	0	0	89
2378.4	ψ_{67}	0	0	0	0	1	0	0	1	0	0	0	0	5	75	4	0	0	0	1	0	0	0	0	0	0	0	0	0	90
2414.1	ψ_{72}	0	0	0	0	0	5	0	0	0	0	0	0	52	8	24	1	0	0	0	0	0	0	0	0	0	0	0	0	94
2458.2	ψ_{74}	0	0	0	0	0	0	0	0	0	1	0	0	1	1	0	81	0	0	0	0	0	2	1	0	0	0	0	0	90
2513.4	ψ_{80}	0	0	0	0	0	2	4	0	1	0	0	0	19	0	58	1	0	0	0	0	0	0	0	0	0	0	0	0	90
2570.8	ψ_{87}	0	0	0	0	0	0	1	0	0	0	0	0	0	0	0	0	72	0	1	0	0	0	0	0	0	0	0	9	85
2602.5	ψ_{91}	0	0	0	0	0	0	0	0	0	0	0	0	0	1	0	0	1	38	45	2	0	1	0	0	0	0	0	0	91
2651.0	ψ_{98}	0	0	0	0	0	0	0	0	0	0	0	0	0	0	0	1	0	13	7	21	0	37	3	0	0	0	1	87	

^aRows of variational vibrational wave functions (ψ_i) with energy levels ν_i are decomposed in terms of columns of harmonic oscillator (HO) basis states with reference energy levels ω_i . NMD coefficients in percent; energies in cm^{-1} relative to the corresponding variational or harmonic zero-point vibrational (ZPV) level appearing in row 1 or column 1 of Table IV, respectively.

^bSee footnote b of Table IV. The only difference is that the decomposition was extended to the first 58 A_2 HO states in each row.

provide considerably different VBOs for this molecule; for example, VPT2 and DEWE differ by a factor of 3 and 2 for the anharmonic corrections to the fundamentals 5^1 and 3^1 , respectively. These large discrepancies should be compared to the ability of the refined quartic force field employed to reproduce measured band origins by an average accuracy of 1 cm^{-1} based on the VPT2 treatment.⁴⁴ This also points to the need of using variational results when refining quartic force fields for molecules exhibiting strong and extensive anharmonic resonances. Another peculiar feature of the computed results is that there is a very large positive anharmonicity for the out-of-plane C=C=O bending fundamental, $6^1 \equiv \nu_6(B_1)$, and its overtones, it is $\{+31.4, +66.5, +99.4, +123.2\} \text{ cm}^{-1}$ for the VBOs $\{6^1, 6^2, 6^3, 6^4\}$, showing some irregularity.

As clear from Table III, the variationally computed VBOs deviate substantially from the experimental MARVEL ones (discussion of the MARVEL levels is given in Sec. V). Since

the variational protocol employed uses an exact kinetic energy operator and includes also the complete PES, these discrepancies are the result of slight problems with the empirically adjusted *ab initio* quartic force field approximation of the PES (Ref. 44) employed in this study. Nevertheless, it is more important to emphasize that the discrepancies are only on the order of a few cm^{-1} , making all semi-quantitative conclusions of this study about the rovibrational characteristics of the ketene molecule valid.

Of the four vibrational resonance interactions identified in Table IX of Ref. 44, three and one within the A_1 and B_2 irreducible representations, respectively, the two lower-energy ones can be investigated here: the tetrad ($\nu_4, 2\nu_5, 2\nu_6, \nu_5 + \nu_6$) at $1100\text{--}1200 \text{ cm}^{-1}$ and the diad ($\nu_3, \nu_8 + \nu_9$) at about 1410 cm^{-1} . Our NMD analysis presented in Table IV clearly confirms the existence of both resonance schemes.

For the Fermi resonance tetrad, the present variational and the previous VPT2 results⁴⁴ show moderate agreement,

TABLE VIII. Active database (MARVEL) and variational quantum mechanical (DEWE) rotational-vibrational energy levels (cm^{-1}) for $J = 1-3$ for $\text{H}_2^{12}\text{C}=\text{C}=\text{O}$ in order of increasing J and energy for the vibrational states GS, $9^1 \equiv \nu_9$, $6^1 \equiv \nu_6$, and $5^1 \equiv \nu_5$, with asymmetric-top rotational labels ($J K_a K_c$), symmetry (S) information, and MARVEL classification (Class., see text for details) and uncertainties (U, 10^{-6}cm^{-1}). The DEWE-VS-DEWE deviations (Δ , cm^{-1}) are reported under DEWE, in parentheses. The size of the vibrational basis for the DEWE computations is $10 \times 10 \times 10 \times 8 \times 8 \times 6 \times 6 \times 6$, that is 8×10^7 , while that of the DEWE-VS computations is 10^2 .

J	K_a	K_c	GS		ν_9		ν_6		ν_5									
			S	Class.	MARVEL [U]	DEWE(Δ)	S	Class.	MARVEL [U]	DEWE(Δ)	S	Class.	MARVEL [U]	DEWE(Δ)				
1	0	1	A_2	A	0.6741 [1]	0.67 (0.01)	B_1	A	440.0612 [231]	440.06 (0.01)	B_2	A	526.7454 [224]	526.72 (0.04)	B_2	A	588.1028 [226]	588.09 (0.02)
1	1	1	B_1	A	9.7395 [1]	9.81 (0.08)	A_2		...	447.28 (0.10)	A_1	B	536.0447 [387]	536.58 (0.13)	A_1		598.3116 [273]	598.05 (0.28)
1	1	0	B_2	A	9.7521 [1]	9.82 (0.08)	A_1		...	447.30 (0.11)	A_2		...	536.59 (0.15)	A_2		598.3229 [358]	598.06 (0.32)
2	0	2	A_1	A	2.0223 [1]	2.02 (0.01)	B_2	A	441.4109 [216]	441.41 (0.01)	B_1	A	528.0947 [226]	528.07 (0.03)	B_1	A	589.4521 [220]	589.43 (0.03)
2	1	2	B_2	A	11.0750 [1]	11.15 (0.07)	A_1		...	448.62 (0.10)	A_2	A	537.3827 [384]	537.92 (0.15)	A_2	B	599.6491 [261]	599.38 (0.28)
2	1	1	B_1	A	11.1128 [1]	11.18 (0.08)	A_2		...	448.66 (0.11)	A_1		...	537.95 (0.13)	A_1	B	599.6843 [354]	599.42 (0.32)
2	2	1	A_2	A	38.3011 [164]	38.58 (0.29)	B_1		470.4844 [355]	470.65 (0.36)	B_2		565.0305 [299]	567.17 (0.44)	B_2		630.2861 [316]	629.34 (1.00)
2	2	0	A_1	A	38.3001 [463]	38.58 (0.29)	B_2		470.4845 [340]	470.65 (0.39)	B_1		565.0305 [345]	567.17 (0.57)	B_1		630.2863 [290]	629.34 (1.15)
3	0	3	A_2	A	4.0446 [1]	4.04 (0.01)	B_1	B	443.4389 [215]	443.44 (0.01)	B_2	B	530.1176 [281]	530.09 (0.04)	B_2	B	591.4766 [221]	591.46 (0.03)
3	1	3	B_1	A	13.0783 [1]	13.15 (0.07)	A_2		...	450.63 (0.10)	A_1	B	539.3884 [381]	539.92 (0.16)	A_1	B	601.6561 [256]	601.38 (0.29)
3	1	2	B_2	A	13.1539 [1]	13.23 (0.07)	A_1		...	450.71 (0.11)	A_2		...	539.99 (0.13)	A_2		601.7264 [354]	601.46 (0.32)
3	2	2	A_1	A	40.3230 [164]	40.60 (0.29)	B_2	B	472.5122 [352]	472.67 (0.37)	B_1	B	567.0534 [298]	569.19 (0.44)	B_1	B	632.3104 [315]	631.36 (1.01)
3	2	1	A_2	A	40.3221 [463]	40.60 (0.29)	B_1	B	472.5123 [337]	472.67 (0.40)	B_2	B	567.0535 [345]	569.19 (0.57)	B_2	B	632.3106 [286]	631.36 (1.15)
3	3	1	B_1	B	85.6354 [168]	86.27 (0.64)	A_2		...	510.13 (0.79)	A_1		612.4090 [527]	616.96 (1.12)	A_1		...	681.34 (2.12)
3	3	0	B_2	A	85.6360 [142]	86.27 (0.64)	A_1		...	510.13 (0.86)	A_2		612.4081 [682]	616.96 (1.41)	A_2		...	681.35 (2.43)

TABLE IX. Selected higher- J ($J \geq 4$) variational quantum mechanical (DEWE-VS) rotational-vibrational energy levels (cm^{-1}) which have active database (MARVEL) counterparts for $\text{H}_2^{12}\text{C} = ^{12}\text{C} = ^{16}\text{O}$ in order of increasing J and energy for the vibrational states GS, $9^1 \equiv \nu_9$, $6^1 \equiv \nu_6$, and $5^1 \equiv \nu_5$, with asymmetric-top rotational labels ($J K_a K_c$), symmetry (S) information, and MARVEL classification (Class.) and uncertainties (U, 10^{-6}cm^{-1}). See Supplementary Material⁹⁶ for the full Table IX containing 238 rows.

J	$K_a K_c$	S	GS		ν_9		ν_6		ν_5								
			Class.	MARVEL [U]	Class.	MARVEL [U]	Class.	MARVEL [U]	Class.	MARVEL [U]							
4	0 4	A_1	A	6.7408 [1]	6.74	B_2	B	446.1430 [137]	446.15	B_1	B	532.8153 [146]	532.82	B_1	B	594.1760 [144]	594.17
4	1 4	B_2	A	15.7494 [1]	15.89									A_2	B	604.3319 [256]	604.33
4	1 3	B_1	A	15.8753 [1]	16.01												
4	2 3	A_2	A	43.0189 [164]	43.58			B_2	B	569.7509 [197]	572.45	B_2	B	635.0096 [164]	635.05		
4	2 2	A_1	A	43.0191 [184]	43.58			B_1	B	569.7508 [169]	572.32	B_1	B	635.0115 [266]	635.20		
4	3 2	B_2	A	88.3307 [168]	89.60												
4	3 1	B_1	A	88.3312 [142]	89.60			A_1	B	615.1058 [343]	620.77						
5	0 5	A_2	A	10.1110 [1]	10.11	B_1	B	449.5228 [132]	449.53	B_2	B	536.1874 [140]	536.19	B_2	B	597.5500 [140]	597.55
5	1 5	B_1	A	19.0882 [1]	19.23												
5	1 4	B_2	A	19.2770 [1]	19.42												
5	2 4	A_1	A	46.3887 [164]	46.95			B_1	B	573.1224 [107]	575.83	B_1	B	638.3833 [161]	638.43		
5	2 3	A_2	A	46.3892 [184]	46.95			B_2	B	573.1225 [83]	575.69	B_2	B	638.3854 [264]	638.57		
5	3 3	B_1	A	91.6997 [168]	92.97			A_1	B	618.4756 [305]	624.43						
5	3 2	B_2	A	91.7003 [142]	92.97			A_2	B	618.4765 [339]	624.14						
5	4 2					B_2	B	569.0673 [563]	571.21	B_1	B	681.0352 [545]	691.34	B_1	B	760.1568 [580]	760.91
5	4 1	A_2	B	155.0751 [420]	157.35	B_1	B	569.0685 [607]	571.32	B_2	B	681.0364 [590]	690.83	B_2	B	760.1577 [653]	761.45
5	5 1	B_2	A	236.4289 [505]	240.04												
5	5 0	B_1	A	236.4301 [554]	240.04												
6	0 6	A_1	A	14.1551 [1]	14.16	B_2	B	453.5782 [131]	451.28	B_1	B	540.2337 [138]	548.18	B_1	B	601.5987 [140]	617.70
6	1 6	B_2	A	23.0947 [1]	23.23			A_2	B	549.4172 [255]	558.05	A_2	B	611.6901 [240]	627.79		
6	1 5	B_1	A	23.3590 [1]	23.50									A_1	B	611.9362 [188]	628.08
6	2 5	A_2	A	50.4324 [164]	50.99	B_1	B	482.6511 [181]	480.87	B_2	B	577.1682 [190]	587.82	B_2	B	642.4317 [160]	658.58
6	2 4	A_1	A	50.4334 [184]	50.99	B_2	B	482.6521 [177]	480.90	B_1	B	577.1687 [163]	587.68	B_1	B	642.4342 [265]	658.73
6	3 4	B_2	A	95.7426 [168]	97.01			A_2	B	622.5204 [303]	636.42						
6	3 3	B_1	A	95.7432 [142]	97.01			A_1	B	622.5213 [338]	636.13						
6	4 3					B_1	B	573.1209 [562]	572.96	B_2	B	685.0786 [544]	703.33	B_2	B	764.2030 [580]	781.06
6	4 2	A_1	B	159.1166 [420]	161.39	B_2	B	573.1221 [606]	573.06	B_1	B	685.0797 [589]	702.82	B_1	B	764.2031 [702]	781.60
6	5 2	B_2	A	240.4686 [505]	244.08												
6	5 1	B_1	A	240.4697 [554]	244.08												
7	0 7	A_2	A	18.8730 [1]	18.87	B_1	B	458.3092 [133]	456.01	B_2	B	544.9542 [140]	552.91	B_2	B	606.3220 [141]	622.42
7	1 7	B_1	A	27.7688 [1]	27.91					A_1	B	554.0971 [254]	562.73	A_1	B	616.3726 [240]	632.47
7	1 6	B_2	A	28.1213 [1]	28.26									A_2	B	616.7007 [185]	632.84
7	2 6	A_1	A	55.1500 [164]	55.71	B_2	B	487.3822 [182]	485.60	B_1	B	581.8882 [190]	592.54	B_1	B	647.1547 [162]	663.30
7	2 5	A_2	A	55.1517 [184]	55.71	B_1	B	487.3843 [174]	485.64	B_2	B	581.8892 [164]	592.41	B_2	B	647.1479 [271]	663.45
7	3 5	B_1	A	100.4593 [168]	101.73					A_1	B	627.2393 [303]	641.14				
7	3 4	B_2	A	100.4599 [142]	101.73					A_2	B	627.2402 [339]	640.85				
7	4 4					B_2	B	577.8502 [562]	577.69	B_1	B	689.7958 [544]	708.05				
7	4 3	A_2	A	163.8316 [420]	166.11	B_1	B	577.8513 [606]	577.80	B_2	B	689.7969 [589]	707.54				
7	5 3	B_1	A	245.1815 [505]	248.79												
7	5 2	B_2	A	245.1826 [554]	248.80												
8	0 8	A_1	A	24.2645 [1]	24.27	B_2	B	463.7157 [138]	461.42	B_1	B	550.3487 [144]	558.30	B_1	B	611.7197 [145]	627.81
8	1 8	B_2	A	33.1106 [1]	33.25					A_2	B	559.4454 [256]	568.08				
8	1 7	B_1	A	33.5638 [1]	33.70									A_1	B	622.1457 [187]	638.28
8	2 7	A_2	A	60.5415 [217]	61.10					B_2	B	587.2824 [194]	597.94	B_2	B	652.5524 [166]	668.69
8	2 6	A_1	A	60.5443 [184]	61.10	B_2	B	492.7927 [175]	491.05	B_1	B	587.2843 [168]	597.80	B_1	B	652.5465 [276]	668.84
8	3 6	B_2	A	105.8498 [168]	107.12												
8	3 5	B_1	A	105.8503 [142]	107.12					A_1	B	632.6332 [341]	646.24				
8	4 5									B_2	B	695.1868 [545]	713.44				
8	4 4	A_1	A	169.2202 [420]	171.49					B_1	B	695.1879 [591]	712.93				
8	5 4	B_2	A	250.5676 [505]	254.18												
8	5 3	B_1	A	250.5687 [554]	254.18												
9	0 9	A_2	A	30.3296 [1]	30.33												
10	0 10	A_1	A	37.0679 [220]	37.07												
11	0 11	A_2	A	44.4796 [220]	44.48												
12	0 12	A_1	A	52.5644 [220]	52.57												

TABLE IX. (Continued)

J	K_a	K_c	S	Class.	GS		ν_9		ν_6		ν_5	
					MARVEL [U]	DEWE-VS	S	Class.	MARVEL [U]	DEWE-VS	S	Class.
13	0	13	A_2	A	61.3220 [220]	61.32						
14	0	14	A_1	A	70.7524 [313]	70.75						
15	0	15	A_2	A	80.8552 [313]	80.86						
20	0	20	A_1	A	141.4475 [576]	141.45						
25	0	25	A_2	A	218.8099 [789]	218.82						
30	0	30	A_1	B	312.9006[1398]	312.92						
35	1	35	B_1	A	429.4011 [637]	429.57						
39	1	38	B_2	B	539.1255 [857]	539.27						
45	0	45	A_2			695.08	B_1	1133.92	B_2	1230.17	B_2	1299.51
50	0	50	A_1			855.58	B_2	1294.72	B_1	1391.01	B_1	1460.32

the “measured” ones (see supplementary material⁹⁶). This is most likely due to deficiencies of the force field used as a model of the PES of ketene.

Since this is the first time we use the vibrational subspace reduction technique, it is worth comparing the energies obtained from a computation with the complete vibrational space of size 8×10^7 (DEWE in Table VIII, see also Sec. II A), performed up to $J = 3$, to those obtained with a reduced vibrational space of dimension 10^2 , constructed according to Sec. II E (DEWE-VS in Tables VIII and IX). In spite of the 10^6 -fold reduction of the size of the rovibrational basis and the corresponding reduction in storage and other resources required to perform the computations, the overall agreement of the first few hundred rovibrational states is better than 1 cm^{-1} . Thus, the error introduced due to this sophisticated truncation of the vibrational space is less than the uncertainty of the underlying PES. The accuracy of the rovibrational energy levels obtained within the DEWE-VS protocol could easily be increased further by including more vibrational eigenstates in the computation. This would preferentially include all the fundamentals of the molecule and all states in between. Naturally, by increasing the size of the vibrational subspace in the second stage of the rovibrational computation, the rovibrational limit corresponding to the complete set of the original primitive vibrational basis functions is approached.

V. MARVEL ENERGY LEVELS

In order to improve our understanding of the measured spectra and validate the experimental assignments proposed for ketene, we analyzed simultaneously all the experimental line information available to us,^{9,12,13,15,19,24,25,40} indicated in Table II. The MARVEL protocol employed for this purpose proved to be successful for a similar analysis of the rovibrational states of several water isotopologues.^{61–63,67} During the present study, we utilized altogether 3982 measured and assigned rovibrational transitions of $\text{H}_2^{12}\text{C}=\text{C}=\text{O}$. Due to nuclear spin symmetry, these transitions form part of two main SNs, ortho and para. The selection rules governing the transitions are given in the supplementary material.⁹⁶

We had two main difficulties with the measured data. First, in many of the original publications the uncertainties

of the measured transitions were not given explicitly. Therefore, we had to assign reasonable uncertainties to several transitions based on the best available information deduced from the original sources. This, however, is not a serious problem as MARVEL adjusts, via robust reweighting, the uncertainties attached to the transitions until self-consistency within the database is achieved. Second, as almost always happens with measured transitions, some of them are not part of the main networks but are part of floating spectroscopic networks (FSNs) or are themselves orphans. Since orphan energy levels and those taking part in FSNs cannot be validated, only 3194 transitions could be validated in this work. Transitions which could not be validated are indicated in Table II source by source.

The ortho and the para SNs contain 2489 and 705 observed transitions and 1251 and 471 MARVEL energy levels, respectively. The MARVEL energy levels of A and B quality go up to $J = 39$ for the vibrational ground state and up to $J = 8$ for the other states. Most highly excited rotational and rovibrational energy levels take part in only a single measured transition. Thus, their accuracy remains uncertain even after the MARVEL validation procedure.

Due to the sparsity of measurements for parent ketene, there are relatively few energy levels of A quality for all but the ground vibrational state (cf. Tables VIII and IX). Thus, since in Tables VIII and IX only MARVEL levels of A and B quality are given, for the excited vibrational states there are plenty of missing levels under the heading MARVEL. The computed levels of C quality should be handled with special care: they may be inaccurate as they are determined by insufficient experimental information, by just a single measured and assigned transition. Thus, though they are given in the supplementary material,⁹⁶ they should be used only with caution.

Figure 2 presents a comparison of absolute differences, given on a semi-logarithmic scale and as a function of the energy of the levels, between the pure rotational MARVEL energy levels of this study and those reported in the CDMS database⁴³ and determined via an effective Hamiltonian based on fitted spectroscopic parameters. Note that energy values having K_a larger than 5 are missing from the figure as no validated experimental data, and thus no MARVEL energy levels, are available for them. The figure clearly shows deviations between the two sets of results. Since the MARVEL energy

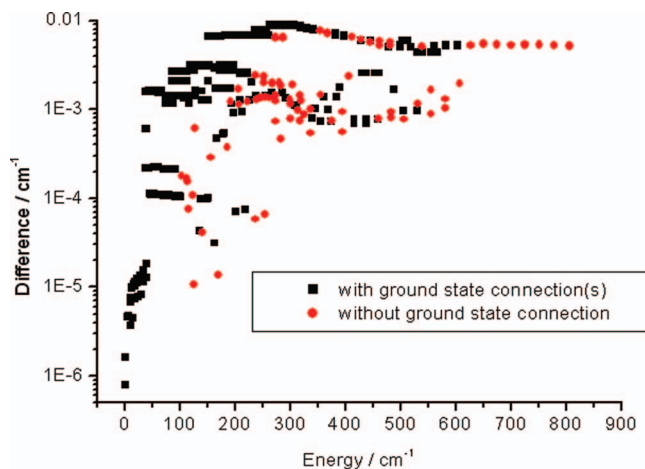


FIG. 2. Absolute differences, on a semi-logarithmic scale, between the pure rotational MARVEL energy levels obtained in this study and those levels reported in the CDMS database (Ref. 43) as a function of the energy of the level.

levels involved in creation of the figure are not only of A and B quality, it cannot be concluded that they present better representation for these levels. Only further experimental studies and a new list of relevant assigned transitions would be able to solve this problem.

VI. NEW ASSIGNMENTS

The apodized resolution in the mid-infrared high resolution IR gas-phase spectra⁹⁷ was ~ 0.004 cm^{-1} , and the relative frequency calibration accuracy was better than 0.001 cm^{-1} as determined by comparison with extensive, known ground state combination differences (CD).³⁷ The absolute wavenumbers have errors smaller than the apodized resolution, a conservative estimate is 0.001 cm^{-1} . These spectra contain several thousand lines, and a sizeable proportion of these are difficult to assign using ground-state CDs, partly because of their low intensity or location in very congested spectral areas, and partly as combination differences require

additional transitions involving some of the levels that are also involved in the transitions to be assigned. (The method of combination differences makes use of the fact that some transitions share a common level). In addition, there are localized resonances in the spectra that perturb regularity. Thus, there is a great need of an independently determined set of rotation-vibration energy levels to facilitate line identification. Such levels of high quality have been obtained in this work using the MARVEL technique validated via the variational nuclear motion DEWE-VS results. The complete list of MARVEL energy levels is presented in the supplementary material.⁹⁶ The presently available energy levels allow a host of new assignments relative to those obtained in previous works.^{21–23} Note also that the vibration-rotation transitions used in Refs. 22 and 23 were not published there explicitly.

We have searched the FTIR spectra⁹⁷ of ketene for regions that had previously not been analyzed by the usual CD methods and thus were not used in perturbation calculations by least-squares fits. In what follows two specific series are given involving lines of rotational-vibrational branches of two fundamentals. In subsequent work, we shall publish a greater number of new spectral assignments for other, so-far not analyzed vibration-rotation transitions for the ketene molecule. The specific examples of newly assigned sets of transitions are given in Table X, which convincingly show the great utility of experimental-quality MARVEL energy levels to make progress in assigning a high-resolution spectrum.

The first branch is the ${}^1R_1(J)$ series of the $\nu_5 \equiv 5^1$ vibrational fundamental that extends from 621.24 to 627.75 cm^{-1} for lines involving lower state $J = 2$ up to $J = 11$ (10 lines). The assignment of this clearly visible series was not attempted earlier due to lack of CD transition partners. These lines occur in a medium congested region but are clearly identifiable due to their narrow profiles and no lines in their close neighbourhood. The differences between the MARVEL and experimental lines are nowhere greater than a couple of times 10^{-4} cm^{-1} ; thus, the line identifications are unique. (Note also that although we give in Table X a comparison for all 10 lines, only a single MARVEL prediction suffices for definitive

TABLE X. New line identifications, based on MARVEL energy levels and associated transitions, of two series of lines ($GS-J_{1J} - 5^1-(J+1)_{2J}$ for ν_5 and $GS-J_{1J} - 8^1-(J+1)_{0(J+1)}$ for ν_8) in the infrared spectrum of ketene, with line data in cm^{-1} .

ν_5	Expt. transition ^a	MARVEL prediction	DEWE-VS ^b	ν_8	Expt. transition ^a	MARVEL prediction	DEWE-VS ^c
${}^1R_1(2)$	621.2357(20)	621.2354(2)	621.2353	${}^pR_1(5)$	972.7856(10)	972.7855(4)	972.7862
${}^1R_1(3)$	621.9312(20)	621.9312(2)	621.9311	${}^pR_1(8)^d$	974.9959(20)	974.9954(4)	974.9949
${}^1R_1(4)$	622.6339(20)	622.6339(2)	622.6339	${}^pR_1(11)^d$	977.2859(20)	977.2858(4)	977.2866
${}^1R_1(5)$	623.3436(20)	623.3435(2)	623.3436				
${}^1R_1(6)$	624.0602(20)	624.0600(2)	623.0603				
${}^1R_1(7)$	624.7835(20)	624.7836(2)	624.7838				
${}^1R_1(8)$	625.5141(20)	625.5150(4)	625.5143				
${}^1R_1(9)$	626.2517(20)	626.2519(4)	626.2518				
${}^1R_1(10)$	626.9962(20)	626.9962(4)	626.9962				
${}^1R_1(11)$	627.7478(20)	627.7474(3)	627.7473				

^aSee beginning of Sec. VI for the discussion of experimental uncertainties.

^bObtained from the directly computed first-principles results via the following quadratic correction form fitted to all MARVEL – DEWE-VS differences: $-16.013366 + 0.000759J + 0.000143J^2$.

^cObtained from the directly computed first-principles results via the following quadratic correction form fitted to all ($J = 5-13$) MARVEL – DEWE-VS differences: $-5.233293 + 0.002764J - 0.001535J^2$.

^dSlightly blended line.

assignments using standard spectroscopic techniques based on series regularity for all unperturbed lines in the series having sufficient intensity and no line blending.)

The next series is the ${}^P R_1(J)$ branch of the fundamental vibration $\nu_8 \equiv 8^1$. This branch is located between 972.78 and 978.87 cm^{-1} and contains clearly resolved rotational features, characterized with J values ranging from 5 to 13. Three new lines have been assigned and all show outstanding agreement with the MARVEL predicted transitions. Other members of this series ($J = 5\text{--}13$) have been identified before and were included in the MARVEL analysis.

Based on the demonstrated success of MARVEL-based assignment of the infrared spectrum of ketene, we plan to publish a large number of new spectral assignments for many other, so far not analyzed vibration-rotation transitions in a subsequent work.

VII. CONCLUSIONS

A joint computational and empirical high-resolution molecular spectroscopy protocol is designed, implemented, and advocated for a systematic and detailed understanding of the internal dynamics of medium-sized semi-rigid molecules. This incorporates earlier work on the variational computation of vibrational energy levels and wave functions using the exact Eckart–Watson kinetic energy operator (DEWE),^{72,73} the computation and analysis of rovibrational energy levels (via the normal-mode decomposition (NMD) and rigid-rotor decomposition (RRD) protocols yielding zeroth-order quantum numbers to characterize the levels),⁵³ as well as a Hamiltonian-free line-inversion protocol (MARVEL) (Ref. 67) developed for a systematic construction of empirical energy levels and transitions ordered in a SN.⁹⁸ In order to employ the protocol for the detailed understanding of the notoriously complex high-resolution spectrum of the parent isotopologue of the 5-atomic ketene molecule, the test molecule of this study, further developments of the variational algorithms were necessary.

First, the DEWE program package^{72,73} was extended with the efficient, full-dimensional variational computation of rovibrational energy levels. Second, the symmetry-adapted Lanczos algorithm was expanded to the case of Abelian molecular symmetry groups with characters $+1$ and -1 in order to allow symmetry-selected computation of not only the vibrational, but also the rovibrational states within the Lanczos procedure. Third, a highly efficient VS reduction method was introduced to reduce the giant vibrational space spanned by the primitive vibrational basis functions and to make rovibrational computations of energy levels and wave functions feasible for high J values accessed by experiments. For example, in the case of ketene, a 10^6 -fold reduction in the size of the vibrational basis was employed which, when the vibrational basis is combined with rigid-rotor eigenfunctions, provided rovibrational energy levels deviating less than 1 cm^{-1} from the results of a complete vibrational basis computation and resulted in energy levels up to $J = 50$. Finally, a general symmetry-determination procedure was devised for the characterization of high- J states obtained within the DEWE-VS

computation. It is anticipated that the DEWE program package will be employed for a systematic study of the rotational-vibrational spectra of 6–7 atom molecules in the very near future.

The presented variational nuclear motion computations utilized a quartic force field⁴⁴ for the representation of the ground-state PES of ketene. The computations resulted in the following conclusions regarding the PES. The variational energy levels obtained clearly indicate that anharmonic force fields adjusted via VPT2 protocols may not have near the same accuracy in a variational treatment as they showed in the simple VPT2 protocol, especially if the spectrum of the molecule is affected by a large number of resonances. This points toward the need to obtain a more accurate representation of the PES of the ketene molecule. There are at least two important reasons why the determination of an accurate semiglobal PES for ketene was not pursued. First, until now there was no code allowing the use of such a PES with an exact kinetic energy operator for the variational computation of the high-lying rovibrational energies and wave functions. Second, there was no comprehensive experimental database containing measured and assigned transitions, which required critical validation and showed the need and the possibility for updates. These are basic requirements to allow the adjustment of a PES of a semirigid molecule. Now that these requirements are fulfilled, it can be expected that development of an accurate PES for the ground electronic state of ketene will be pursued.

As to the spectroscopy of ketene, the present variational study offers several interesting results. The detailed NMD tables obtained identify those vibrational bands, which are greatly affected by resonances and those which are not. It is unclear, for example, based on variational quantum chemical computations alone, whether the $3^1 = \nu_3(A_1)$ fundamental of parent ketene is at 1402 or at 1416 cm^{-1} . Based on qualitative arguments, we prefer the lower assignment. The clear-cut RRD values allow for an unambiguous assignment of rigid-rotor quantum numbers to the great majority of rovibrational states. These should be highly useful in future experimental studies of the ketene molecule.

The collection of known rovibrational transitions analysed in this work via the MARVEL protocol confirms the correctness of a sizeable group of experimental assignments for the parent isotopologue of ketene. The accurate MARVEL energy levels obtained can be used to make a number of new assignments. Two examples are given in this work involving 13 new transitions, 10 for the $5^1-(J+1)_{2,J} \leftarrow \text{GS-}J_{1,J}$ branch at about 625 cm^{-1} and 3 for the $8^1-(J+1)_{0,J+1} \leftarrow \text{GS-}J_{1,J}$ branch at about 975 cm^{-1} . Based on the availability of a high-resolution mid-IR spectrum, the MARVEL energy levels, and the DEWE-VS results, lot more assignments for parent ketene are expected to be made in the near future, and these will be published in a separate paper.

ACKNOWLEDGMENTS

This research was carried out with the financial help of the Hungarian Scientific Research Fund (OTKA, Grant Nos. K72885 and NK83583), ERA-Chemistry, and the EU

FP6 QUASAAR program. The European Union and the European Social Fund have also provided financial support to this project under Grant No. TÁMOP-4.2.1./B-09/KMR-2010-0003. The authors are grateful to Dr. H. S. P. Müller for his help concerning the ketene data deposited in the CDMS. Dr. A. Guarnieri's help related to the TNA40 data is also acknowledged.

- ¹P. Jensen and P. R. Bunker, *Computational Molecular Spectroscopy* (Wiley, New York, 2000).
- ²G. Herzberg, *Molecular Spectra and Molecular Structure I–III* (Van Nostrand, New York, 1945).
- ³D. Papoušek and M. R. Aliev, *Molecular Vibrational-Rotational Spectra* (Elsevier, Amsterdam, 1982).
- ⁴J. K. G. Watson, *Mol. Phys.* **15**, 479 (1968).
- ⁵J. K. G. Watson, *Mol. Phys.* **19**, 465 (1970).
- ⁶C. Eckart, *Phys. Rev.* **47**, 552 (1935).
- ⁷H. Kopper, *Z. Phys. Chem. B* **34**, 396 (1936).
- ⁸F. Hegelund, J. Kauppinen, and F. Winther, *Mol. Phys.* **61**, 261 (1987).
- ⁹R. Escríbano, J. L. Domenech, P. Cancio, J. Ortigoso, J. Santos, and D. Bermejo, *J. Chem. Phys.* **101**, 937 (1994).
- ¹⁰H. Gershinowitz and E. B. Wilson, *J. Chem. Phys.* **5**, 500 (1937).
- ¹¹B. Bak, E. S. Knudsen, E. Madsen, and J. Rastrup-Andersen, *Phys. Rev.* **79**, 190 (1950).
- ¹²H. R. Johnson and M. W. P. Strandberg, *J. Chem. Phys.* **20**, 687 (1952).
- ¹³B. Bak and F. A. Andersen, *J. Chem. Phys.* **22**, 1050 (1954).
- ¹⁴L. Nemes and M. Winnewisser, *Z. Naturforsch.* **31A**, 272 (1976).
- ¹⁵L. Nemes, J. Demaison, and G. Włodarczak, *Acta Phys. Hung.* **61**, 135 (1987).
- ¹⁶D. H. Sutter and H. Dreizler, *Z. Naturforsch.* **55A**, 695 (2000).
- ¹⁷C. B. Moore and G. C. Pimentel, *J. Chem. Phys.* **38**, 2816 (1963).
- ¹⁸P. Cox and A. S. Ebbitt, *J. Chem. Phys.* **38**, 1636 (1963).
- ¹⁹J. W. C. Johns, J. M. R. Stone, and G. Winnewisser, *J. Mol. Spectrosc.* **42**, 523 (1972).
- ²⁰A. Guarnieri and A. Huckauf, *Z. Naturforsch.* **58A**, 275 (2003).
- ²¹M. C. Campina, E. Domingo, M. P. Fernandez-Liencres, R. Escríbano, and L. Nemes, *Anales de Quimica-Internat. Ed.* **94**, 23 (1998).
- ²²M. Gruebele, J. W. C. Johns, and L. Nemes, *J. Mol. Spectrosc.* **198**, 376 (1999).
- ²³L. Nemes, D. Luckhaus, M. Quack, and J. W. C. Johns, *J. Mol. Struct.* **517–518**, 217 (2000).
- ²⁴B. Strickler, L. Nemes, and M. Gruebele, *J. Mol. Spectrosc.* **219**, 335 (2003).
- ²⁵R. D. Brown, P. D. Godfrey, D. McNaughton, A. P. Pierlot, and W. H. Taylor, *J. Mol. Spectrosc.* **140**, 340 (1990).
- ²⁶B. Fabricant, D. Krieger, and J. S. Muenter, *J. Chem. Phys.* **67**, 1576 (1977).
- ²⁷J. L. Duncan, A. M. Ferguson, J. Harper, and K. H. Tonge, *J. Mol. Spectrosc.* **125**, 196 (1987).
- ²⁸P. D. Mallinson and L. Nemes, *J. Mol. Spectrosc.* **59**, 470 (1976).
- ²⁹W. F. Arendale and W. H. Fletcher, *J. Chem. Phys.* **24**, 581 (1956).
- ³⁰P. E. B. Butler, D. R. Eaton, and H. W. Thompson, *Spectrochim. Acta* **13**, 223 (1958).
- ³¹W. F. Arendale and W. H. Fletcher, *J. Chem. Phys.* **26**, 793 (1957).
- ³²L. Nemes, *J. Mol. Spectrosc.* **72**, 102 (1978).
- ³³F. Winther, F. Hegelund, and L. Nemes, *J. Mol. Spectrosc.* **117**, 388 (1986).
- ³⁴J. L. Duncan and A. M. Ferguson, *Spectrochim. Acta, Part A* **43**, 1081 (1987).
- ³⁵D. H. Sutter and H. Dreizler, *Z. Naturforsch.* **55A**, 695 (2000).
- ³⁶J. L. Duncan, A. M. Ferguson, J. Harper, K. H. Tonge, and F. Hegelund, *J. Mol. Spectrosc.* **122**, 72 (1987).
- ³⁷L. Nemes and J. W. C. Johns, *Acta Phys. Hung.* **74**, 367 (1994).
- ³⁸J. L. Duncan and B. Munro, *J. Mol. Struct.* **161**, 311 (1987).
- ³⁹J. W. C. Johns, L. Nemes, K. M. T. Yamada, T. Y. Wang, J. L. Domenech, J. Santos, P. Cancio, D. Bermejo, J. Ortigoso, and R. Escríbano, *J. Mol. Spectrosc.* **156**, 501 (1992).
- ⁴⁰R. Hinze, H. Zerbe-Foese, J. Doose, and A. Guarnieri, *J. Mol. Spectrosc.* **176**, 133 (1996).
- ⁴¹A. P. Cox, L. F. Thomas, and J. Sheridan, *Spectrochim. Acta* **15**, 542 (1959).
- ⁴²R. Escríbano, J. Ortigoso, E. Cution, and I. Garcia-Moreno, *J. Chem. Phys.* **93**, 9208 (1990).
- ⁴³H. S. P. Müller, S. Thorwirth, D. A. Roth, and G. Winnewisser, *Astron. Astrophys.* **370**, L49–L52 (2001); H. S. P. Müller, F. Schlöder, J. Stutzki, and G. Winnewisser, *J. Mol. Struct.* **742**, 215–227 (2005); For data on parent ketene, see the web page <http://www.ph1.uni-koeln.de/cgi-bin/cdmsinfo?file=e042501.cat> (accessed on January 10, 2011).
- ⁴⁴A. L. L. East, W. D. Allen, and S. J. Klippenstein, *J. Chem. Phys.* **102**, 8506 (1995).
- ⁴⁵S. J. Klippenstein, A. L. L. East, and W. D. Allen, *J. Chem. Phys.* **105**, 118 (1996).
- ⁴⁶A. G. Császár, in *The Encyclopedia of Computational Chemistry*, edited by P. v. R. Schleyer, (Wiley, Chichester, 1998), Vol. 1, pp. 13–30.
- ⁴⁷I. M. Mills, in *Molecular Spectroscopy: Modern Research*, edited by K. N. Rao and C. W. Mathews (Academic, New York, 1972), Vol. 1, p. 115.
- ⁴⁸H. H. Nielsen, *Rev. Mod. Phys.* **23**, 90 (1951).
- ⁴⁹D. A. Clabo Jr., W. D. Allen, Y. Yamaguchi, R. B. Remington, and H. F. Schaefer III, *Chem. Phys.* **123**, 187 (1988).
- ⁵⁰W. D. Allen, Y. Yamaguchi, A. G. Császár, D. A. Clabo, Jr., R. B. Remington, H. F. Schaefer, *Chem. Phys.* **145**, 427 (1990).
- ⁵¹B. S. Ray, *Z. Phys.* **78**, 74 (1932).
- ⁵²R. S. Mulliken, *J. Chem. Phys.* **23**, 1997 (1955).
- ⁵³E. Mátyus, C. Fábri, T. Szidarovszky, G. Czákó, W. D. Allen, and A. G. Császár, *J. Chem. Phys.* **133**, 034113 (2010).
- ⁵⁴P. G. Szalay, A. G. Császár, and L. Nemes, *J. Chem. Phys.* **105**, 1034 (1996).
- ⁵⁵A. G. Császár and N. C. Handy, *Mol. Phys.* **86**, 959 (1995).
- ⁵⁶I. Garcia-Moreno, E. R. Lovejoy, and C. B. Moore, *J. Chem. Phys.* **100**, 8902 (1994).
- ⁵⁷S. K. Kim, E. R. Lovejoy, and C. B. Moore, *J. Chem. Phys.* **102**, 3202 (1995).
- ⁵⁸S. C. Smith, *Faraday Discuss.* **102**, 17 (1995).
- ⁵⁹S. C. Smith, *Chem. Phys. Lett.* **243**, 359 (1995).
- ⁶⁰A. J. Rasmussen, K. E. Gates, and S. C. Smith, *J. Chem. Phys.* **110**, 1354 (1999).
- ⁶¹A. G. Császár, G. Czákó, T. Furtenbacher, and E. Mátyus, *Ann. Rep. Comput. Chem.* **3**, 155 (2007).
- ⁶²J. Tennyson, P. F. Bernath, L. R. Brown, A. Campargue, M. R. Carleer, A. G. Császár, R. R. Gamache, J. T. Hodges, A. Jenouvrier, O. V. Naumenko, O. L. Polyansky, L. S. Rothman, R. A. Toth, A. C. Vandaele, N. F. Zobov, L. Daumont, A. Z. Fazliev, T. Furtenbacher, I. F. Gordon, S. N. Mikhailenko, and S. V. Shirin, *J. Quantum Spectrosc. Rad. Transfer* **110**, 573 (2009).
- ⁶³J. Tennyson, P. F. Bernath, L. R. Brown, A. Campargue, M. R. Carleer, A. G. Császár, L. Daumont, R. R. Gamache, J. T. Hodges, A. Jenouvrier, O. V. Naumenko, O. L. Polyansky, L. S. Rothman, R. A. Toth, A. C. Vandaele, N. F. Zobov, A. Z. Fazliev, T. Furtenbacher, I. F. Gordon, S.-M. Hu, S. N. Mikhailenko, and B. Voronin, *J. Quant. Spectr. Radiat. Transfer* **111**, 2160 (2010).
- ⁶⁴O. L. Polyansky, A. G. Császár, S. V. Shirin, N. F. Zobov, P. Barletta, J. Tennyson, D. W. Schwenke, and P. J. Knowles, *Science* **299**, 539 (2003).
- ⁶⁵A. G. Császár, W. D. Allen, Y. Yamaguchi, and H. F. Schaefer III, in *Computational Molecular Spectroscopy*, edited by P. Jensen and P. R. Bunker (Wiley, New York, 2000).
- ⁶⁶A. G. Császár, G. Tarczay, M. L. Leininger, O. L. Polyansky, J. Tennyson, and W. D. Allen, in *Spectroscopy from Space*, edited by J. Demaison, K. Sarka, and E. A. Cohen (Kluwer, Dordrecht, 2001), pp. 317–339.
- ⁶⁷T. Furtenbacher, A. G. Császár, and J. Tennyson, *J. Mol. Spectrosc.* **245**, 115 (2007).
- ⁶⁸J.-M. Flaud, C. Camy-Peyret, and J. P. Maillard, *Mol. Phys.* **32**, 499 (1976).
- ⁶⁹M. Born and R. Oppenheimer, *Ann. Phys.* **389**, 457 (1927).
- ⁷⁰M. Born and K. Huang, *Dynamical Theory of Crystal Lattices* (Oxford University Press, New York, 1954).
- ⁷¹P. R. Bunker and P. Jensen, *Molecular Symmetry and Spectroscopy* (NRC, Ottawa, 1998).
- ⁷²E. Mátyus, G. Czákó, B. T. Sutcliffe, and A. G. Császár, *J. Chem. Phys.* **127**, 084102 (2007).
- ⁷³E. Mátyus, J. Šimunek, and A. G. Császár, *J. Chem. Phys.* **131**, 074106 (2009).
- ⁷⁴J. C. Light and T. Carrington, Jr., *Adv. Chem. Phys.* **114**, 263 (2000).
- ⁷⁵N. M. Poulain, M. J. Bramley, T. Carrington, Jr., H. G. Kjaergaard, and B. R. Henry, *J. Chem. Phys.* **104**, 7807 (1996).
- ⁷⁶X.-G. Wang and T. Carrington, *J. Chem. Phys.* **114**, 1473 (2001).
- ⁷⁷R. Chen and H. Guo, *J. Chem. Phys.* **114**, 1467 (2001).

- ⁷⁸B. T. Sutcliffe and J. Tennyson, *Int. J. Quantum Chem.* **39**, 183 (1991).
- ⁷⁹R. N. Zare, *Angular Momentum* (Wiley, New York, 1988).
- ⁸⁰C. Lanczos, *J. Res. Natl. Bur. Stand.* **45**, 255 (1950).
- ⁸¹J. K. Cullum and R. A. Willoughby, *Lanczos Algorithms for Large Symmetric Eigenvalue Computations* (Birkhauser, Boston, 1985).
- ⁸²L. W. Wang and A. Zunger, *J. Chem. Phys.* **100**, 2394 (1994).
- ⁸³I. J. Farkas, I. Derényi, A. L. Barabási, and T. Vicsek, *Phys. Rev. E* **64**, 026704 (2001).
- ⁸⁴J. Grcar, "Analyses of the Lanczos Algorithm and of the Approximation Problem in Richardson's Method," Ph.D. dissertation (University of Illinois, 1981).
- ⁸⁵H. D. Simon, *Math. Comput.* **42**, 115 (1984).
- ⁸⁶K. Wu and H. D. Simon, "Thick-restart Lanczos Method for the Symmetric Eigenvalue problems," Lawrence Berkeley National Laboratory Report No. 41412, 1998.
- ⁸⁷K. Wu, A. Canning, H. D. Simon, and L. W. Wang, *J. Comput. Phys.* **154**, 156 (1999).
- ⁸⁸See <http://software.intel.com/en-us/articles/intel-mkl/> for Intel's Math Kernel, last accessed on February 5, 2011.
- ⁸⁹P. Pulay, G. Fogarasi, G. Pongor, J. E. Boggs, and A. Vargha, *J. Am. Chem. Soc.* **105**, 7037 (1983).
- ⁹⁰W. D. Allen, A. G. Császár, and D. A. Horner, *J. Am. Chem. Soc.* **114**, 6834 (1992).
- ⁹¹G. Czako, T. Furtenbacher, A. G. Császár, and V. Szalay, *Mol. Phys.* **102**, 2411 (2004).
- ⁹²G. Simons, R. G. Parr, and J. M. Finlan, *J. Chem. Phys.* **59**, 3229 (1973).
- ⁹³INTDER2000 is a connected set of FORTRAN programs developed by Allen and co-workers for performing general curvilinear transformations and associated tasks often encountered in the calculation of anharmonic molecular force fields.
- ⁹⁴W. D. Allen, A. G. Császár, V. Szalay, and I. M. Mills, *Mol. Phys.* **89**, 1213 (1996).
- ⁹⁵W. D. Allen and A. G. Császár, *J. Chem. Phys.* **98**, 2983 (1993).
- ⁹⁶See supplementary material at <http://dx.doi.org/10.1063/1.3625404> for the final quartic internal coordinate force field as a representation of the PES of ketene; technical description of the MARVEL tags; technical description of MARVEL quality classifications; a MARVEL input file containing the transitions; MARVEL energy levels; DEWE-VS input and output energy levels for GS, ν_9 , ν_6 , and ν_5 up to $J = 50$; full form of Table IX; and selection rules for parent ketene.
- ⁹⁷These data originated from the laboratory of Dr. John W. C. Johns at the Herzberg Institute of Astrophysics, Ottawa, Canada and were taken using a BOMEM DA3.002 FTIR instrument in 1986. The apodized resolution was $\sim 0.004 \text{ cm}^{-1}$, and the relative frequency calibration accuracy was better than 0.001 cm^{-1} , as determined by comparison with extensive, known ground-state combination differences. The absolute wavenumbers have errors smaller than the apodized resolution. The spectral analysis was performed by L. Nemes.
- ⁹⁸A. G. Császár and T. Furtenbacher, *J. Mol. Spectrosc.* **266**, 99 (2011).